

Improvement Of Load Transient Response Of A Buck Converter Employing Peak Current Mode Control

K. Upendhar¹, L. Srinivas Goud²

1, 2 Aurora engineering college Bhona giri, Andhra pradesh

Abstract

The paper investigates the effect of unity-gain output current- Feed forward in a peak-current-mode-controlled (PCMC) buck converter. A consistent theoretical basis is provided showing that the unity-gain feed forward can improve significantly the load invariance and transient performance of a PCMC buck converter. The non idealities associated to the scheme would, however, deteriorate the obtainable level of invariance. The non idealities can be maintained at acceptable level, and therefore, the scheme would provide a viable method to reduce significantly the load interactions as well as improve the load-transient response. The theoretical predictions are supported with comprehensive experimental evidence both at frequency and time domain as well as comparisons between three different buck converters.

Index Terms—Buck converter, load-current feed forward, output impedance, peak-current-mode control (PCMC).

I. INTRODUCTION

Interconnected regulated power supply systems— known also as distributed power supply (DPS) systems (Fig 1)—are extensively used to supply different electronic loads. The nonlinear nature of the associated regulated converters would make the interconnected systems prone to stability and performance problems. Basically it is a question of the interactions caused by the different impedances [i.e., the output impedance of the source system (Z_o , Fig. 1) and the input impedance of the load system (Z_{in} Fig1)] associated to the specified interface within the system. A natural desire would be to get rid of those interactions. It is well known that the load impedance (i.e Z_{in} Fig.1) may affect adversely the voltage-loop gain of the converter (i.e., the supply converter in Fig. 1). It is claimed explicitly in, and implicitly in and that the load invariance may be achieved by designing the voltage-loop controller in such a way that makes the closed-loop internal output impedance small. According to sound scientific theory, the load interactions are reflected into the converter dynamics via the open-loop internal output impedance. Therefore, it may be obvious that the perfect load invariance at arbitrary load may be achieved only, if the open-loop internal output

impedance is designed to be zero. It was demonstrated in that even the zero open-loop output impedance does not necessarily ensure load invariance, because the load may interact the converter dynamics via the internal input impedance at the presence of the source impedance.

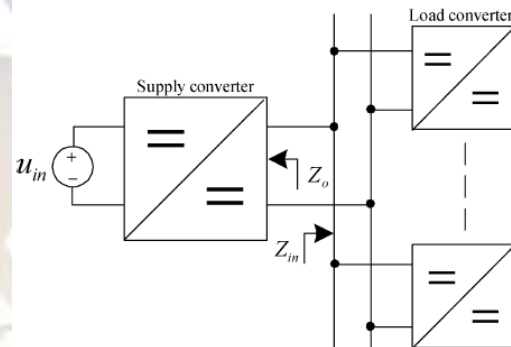


Fig..1 Interconnected regulated system.

The use of output-current feed forward has been demonstrated to improve the output-voltage transient performance for the load-current changes in a hysteretic current-mode-controlled (HCMC) buck converter in. According to the applied theory, the zero output impedance would be achieved by using unity-feed forward gain. The peak-current-mode-controlled (PCMC) buck converter is treated in. The effect of output-current feed forward on the output impedance of the converter is comprehensively analyzed. Close to unity-feed forward gain is stated to give the minimum output impedance. The general conditions for achieving zero output impedance have been derived in. It was stated that the zero output impedance can be implemented in any converter regardless of topology but the validations were only carried out by using a buck converter. A voltage-mode-controlled (VMC) buck converter has been treated in but the theoretical basis for the design approach is not explicitly defined and therefore, the validation of the method is difficult. The experimental load transients shown in imply that the zero output impedance may not be achievable in a boost converter by applying output-current feed forward, i.e., a better transient behavior may be achieved by optimizing the voltage-loop-controller design.

A theoretically consistent treatment of the effect of output current feed forward in a regulated converter is presented in. It defines explicitly the

required conditions for theoretical zero output impedance at open loop based on the well-known transfer functions of the associated converter. According to it, the zero output-impedance conditions are impossible to implement in a converter exhibiting non minimum phase behavior due to the right-hand-plane zero.

The dynamical effect of output-current-feedforward with a unity gain in a peak-current-mode-controlled (PCMC-OCF) buck converter is treated in this paper. The consistent theoretical basis has been provided earlier in. The theoretical predictions are proved by means of experiments both in frequency and time domain. The effect of nonidealities is addressed in detail. Comparisons between VMC, PCMC, and PCMC-OCF buck converters are provided by using the same power stage with different control systems. The results show that the unity-gain output-current-feedforward scheme in a PCMC buck converter is a viable method to improve the load insensitivity. In addition, the PCM control in a buck converter would reduce also the source interactions (i.e., input or source invariance) due to high input-to-output attenuation at open loop and as a consequence also the load interactions via the source impedance.

II. SOURCE-LOAD-INTERACTION MECHANISM

The dynamics of a switched-mode converter is usually represented by means of a set of transfer functions at open loop as defined in (1). The load of the converter is not commonly known, when the converter is designed, produced, and delivered. Therefore, it would be most convenient to give such a set of transfer functions, which only represents the internal dynamics of the converter without the effect of source or load impedances. Such a set is known as an un terminated set, which can be usually measured using an ideal constant-voltage source and an ideal constant-current load [Fig.2(a)]. The set will be known in this paper as a nominal set due to its specific nature representing the pure internal dynamics of the associated converter. The transfer functions constituting the set in (1) can be deduced by means of the variables in the input vector $[\hat{u}_{in} \ \hat{i}_o \ \hat{c}]^T$ and the output vector $[\hat{i}_{in} \ \hat{v}_o]^T$, where \hat{c} denotes the general control variable, respectively. The set in (1) can be equally represented by using a linear two-port model shown in Fig.2(a), which defines also explicitly the used input and output variables in

$$= \begin{bmatrix} Y_{in-o} & T_{oi-o} & G_{ci} \\ G_{io-o} & -Z_{o-o} & G_{co} \end{bmatrix} \begin{bmatrix} \hat{u}_{in} \\ \hat{i}_o \\ \hat{c} \end{bmatrix} \begin{bmatrix} \hat{i}_{in} \\ \hat{v}_o \end{bmatrix} \quad (1)$$

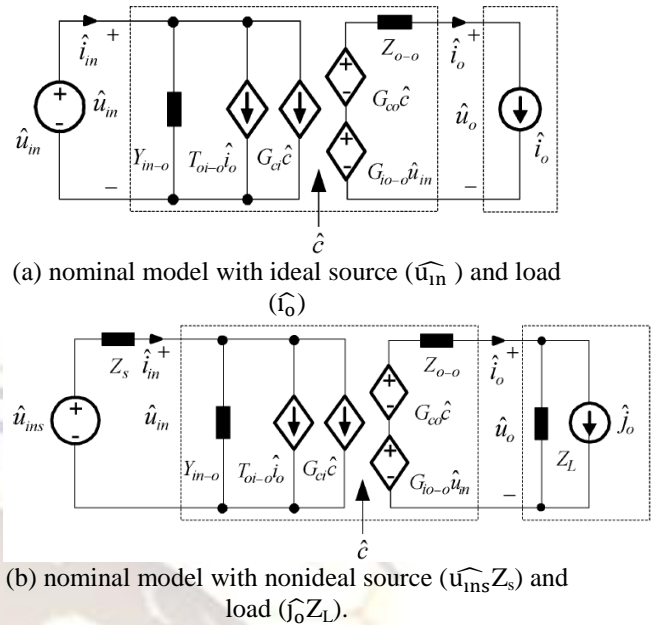


Fig. 2. Linear two-port models

A. Load Interactions

The effect of load impedance [i.e., Z_L in Fig.2(b)] on the dynamics of a converter can be approximated by computing \hat{v}_o and \hat{i}_o from Fig.2(b), when the nonideal load is connected, giving (2). Replacing \hat{v}_o and \hat{i}_o in (1) by means of (2) gives the load-affected dynamical representation of a converter as shown in (3) as a function of the nominal model and the load. The same load-interaction formalism (3) may be also derived using the extra element theorem introduced in by means of the linear two-port model

$$\hat{v}_o = \frac{G_{io-o}\hat{u}_{in} - Z_{o-o}\hat{j}_o + G_{co}\hat{c}}{1 + \frac{Z_{o-o}}{Z_L}} \quad (1)$$

$$\hat{i}_o = \frac{G_{io-o}\hat{u}_{in} + G_{co}\hat{c} + Z_L\hat{j}_o}{Z_L + Z_{o-o}} \quad (2)$$

$$\begin{bmatrix} \hat{i}_{in} \\ \hat{v}_o \end{bmatrix} = \begin{bmatrix} Y_{in-o} + \frac{G_{io-o}T_{oi-o}}{Z_L + Z_{o-o}} & \frac{Z_L T_{oi-o}}{Z_L + Z_{o-o}} & G_{ci} + \frac{G_{ci}T_{oi-o}}{Z_L + Z_{o-o}} \\ \frac{G_{io-o}}{1 + \frac{Z_{o-o}}{Z_L}} & -\frac{Z_{o-o}}{1 + \frac{Z_{o-o}}{Z_L}} & \frac{G_{co}}{1 + \frac{Z_{o-o}}{Z_L}} \end{bmatrix} \times \begin{bmatrix} \hat{u}_{in} \\ \hat{j}_o \\ \hat{c} \end{bmatrix} \quad (3)$$

The control-to-output transfer function is one of the key elements in the voltage-loop gain. Therefore, changes in it would reflect directly changes also in the voltage-loop gain or in the dynamics of the converter. According to (3), the load-affected control-to-output transfer function (i.e., $G_{co} / (1 + \frac{Z_{o-o}}{Z_L})$) would stay intact (i.e., $= G_{co}$), if the internal output impedance $Z_{o-o} = 0$. Similarly, $Y_{in-o} + G_{io-o}T_{oi-o} / (Z_L + Z_{o-o})$ the load-

affected open-loop input admittance (i.e.,) would stay intact (i.e., Y_{in-o}), if the open loop input-to-output transfer function $G_{io-o} = 0$.

B. Source Interactions

The effect of source impedance [i.e., Z_s in Fig.2(b)] on the dynamics of a converter can be approximated by computing \hat{u}_{in} and \hat{i}_{in} from Fig.2(b), when the nonideal source is connected, giving (4). Replacing \hat{u}_{in} and \hat{i}_{in} in (1) by means of (4) gives the source-affected dynamical representation of a converter as shown in (5) as the function of the nominal model and source. $Y_{in-\infty}$ and Y_{in-sc} in (5) are defined in (6), respectively. $Y_{in-\infty}$ is known as an ideal input admittance and Y_{in-sc} as an open-loop short-circuit admittance. Both of the special admittances are load invariant. The ideal input admittance is specific for a given topology but the conduction and control modes do not affect it, i.e., its value can be computed according to (6) by using the voltage-mode transfer functions. The short-circuit admittance is dependent on the control mode, and therefore, the corresponding transfer functions in (6) have to be the nominal transfer functions of the associated topology and control mode.

$$\hat{u}_{in} = \frac{\hat{u}_{ins} - Z_s T_{oi-o} \hat{i}_o - Z_s G_{ci} \hat{c}}{1 + Z_s Y_{in-o}} \tag{4}$$

$$\hat{i}_{in} = \frac{Y_{in-o} \hat{u}_{ins} + T_{oi-o} \hat{i}_o + G_{ci} \hat{c}}{1 + Z_s Y_{in-o}} \tag{4}$$

$$\begin{bmatrix} \hat{u}_{in} \\ \hat{i}_{in} \end{bmatrix} = \begin{bmatrix} \frac{Y_{in-o}}{1 + Z_s Y_{in-o}} & \frac{T_{oi-o}}{1 + Z_s Y_{in-o}} & \frac{G_{ci}}{1 + Z_s Y_{in-o}} \\ \frac{G_{io-o}}{1 + Z_s Y_{in-o}} & \frac{1 + Z_s Y_{in-sc}}{1 + Z_s Y_{in-o}} & \frac{1 + Z_s Y_{in-\infty}}{1 + Z_s Y_{in-o}} \end{bmatrix} \times \begin{bmatrix} \hat{u}_{ins} \\ \hat{i}_o \\ \hat{c} \end{bmatrix} \tag{5}$$

$$Y_{in-\infty} = Y_{in-o} - \frac{G_{io-o} G_{ci}}{G_{co}} \tag{6}$$

$$Y_{in-sc} = Y_{in-o} - \frac{G_{io-o} T_{oi-o}}{Z_{o-o}} \tag{6}$$

According to (5) and (6), the source-affected control-to-output transfer function (i.e., $(1 + Z_s Y_{in-\infty} G_{co}) / (1 + Z_s Y_{in-o})$) and the internal output impedance (i.e., $(1 + Z_s Y_{in-sc}) Z_{o-o} / (1 + Z_s Y_{in-o})$) at open loop would stay intact, if the open-loop input-to-output transfer function $G_{io-o} = 0$. As a summary we may state that a converter having zero output impedance and zero input-to-output transfer function at open loop would provide both load and supply invariance. In practice, perfect load and source invariance may not be achievable due to parasitic circuit elements, circuit nonlinearities, and control delays, etc.

III. ZERO OUTPUT IMPEDANCE

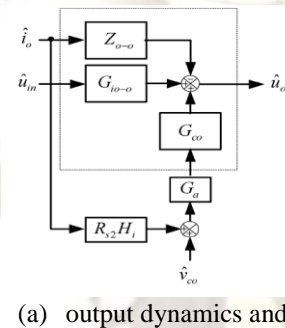
The required output-current-feed forward gain $H_i(s)$ (Fig.3) to achieve theoretically zero open-loop output impedance can be derived from the control-block diagram shown in Fig.3(a), where R_{s2} is the equivalent output-current sensing resistor, and G_a

is the gain factor between the control voltage (\hat{v}_c , Fig.3) and the control signal (\hat{c} , Fig.2) (i.e., $G_a = \frac{\hat{c}}{\hat{v}_c}$). According to Fig.3(a), we can compute the set of transfer functions defining the output dynamics of the converter to be (7). The corresponding set for the input dynamics (8) can be computed from Fig.3 (b), respectively

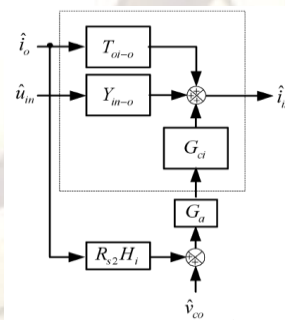
$$\begin{aligned} G_{co-ocf} &= G_a G_{co} \\ Z_{o-o-ocf} &= Z_{o-o} - R_{s2} H_i G_a G_{co} \\ G_{io-o-ocf} &= G_{io-o} \end{aligned} \tag{7}$$

$$\begin{aligned} G_{ci-ocf} &= G_a G_{ci} \\ Y_{in-o-ocf} &= Y_{in-o} \\ T_{oi-o-ocf} &= T_{oi-o} + R_{s2} H_i G_a G_{ci} \end{aligned} \tag{8}$$

According to (7) and (8), the load-current feed forward would affect only the output impedance (Z_{o-o}) and the output-to-input transfer function (T_{oi-o}). All the other transfer functions would stay virtually intact. Similar conclusions are also presented in but the methodology to come up to the conclusions is erroneous as criticized in.



(a) output dynamics and



(b) input dynamics.

Fig. 3. Control-block diagrams for solving the dynamics of a converter with load-current feedforward

The zero-output-impedance condition for $H_i(s)$ can be derived from (7) letting $Z_{o-o-ocf} = 0$, which gives (9). The zero impedance conditions presented in may be the same as (9) but the definitions of the variables used in the corresponding equation are not deterministic and the statement that the derived feed forward gain can be implemented for any converter does not hold: The non minimum-phase converters (e.g., boost and buck-boost) have

right-hand-plane (RHP) zero in the control-to output transfer function, and it cannot be implemented without causing instability. Therefore, theoretically correct feed forward gain (9) may be implemented only for the minimum-phase converters such as a buck converter

$$H_i(s) = \frac{1}{R_{s2}G_a} \cdot \frac{Z_{o-o}}{G_{co}} \quad (8)$$

It may be obvious that the unity-feed forward gain (i.e. $H_i(s)=1$) would be desired due to easiness of implementation. The lack of resonant behavior and rather high low-frequency open-loop output impedance make the PCM-controlled buck converter an optimal medium for achieving low open-loop output impedance by using unity-feed forward scheme. The unity-feed forward scheme in a VM-controlled buck converter does not give desired results due to resonant behavior of the output impedance: The feed forward scheme should be effective at the frequencies close to the resonant frequency of the converter as is implicitly stated in. We do not consider further the methods needed for the other converters to implement the zero or close to zero output impedance but the basis for the methods 1. or their existence may be concluded from (9) by means of appropriate transfer functions.

IV. UNITY FEEDFORWARD SCHEME

The buck converter under consideration is shown in Fig.4 with the relevant power-stage parameters. The nominal transfer functions corresponding to (1) for the PCMC buck converter can be given as shown in (10) and (11) where the duty-ratio

gain $F_m = \frac{D(1-D)}{T_s(2LM_c + (U_{in} + U_D + I_o(r_d - r_{ds}))(D' - D))}$, $q_i = DD'T_s/2L, M_c$, is the slope of the artificial compensation (i.e., for optimal compensation $M_c \approx (U_o + U_D)/2L$ giving $G_{i0-o} = 0$), U_E and r_E are defined in (12). In the case of PCM control, $G_a = \frac{1}{R_{s1}}$, where R_{s1} is the equivalent inductor-current-sensing resistor

$$\begin{bmatrix} Y_{in-o} & T_{oi-o} \\ G_{i0-o} & -Z_{o-o} \end{bmatrix} = \frac{\begin{bmatrix} (D-F_m U_E q_i)(D-F_m I_o)s & (D-F_m I_o)(1+sr_c C) \\ (D-F_m U_E q_i)(1+sr_c C) & -(r_E + F_m U_E + sL)(1+sr_c C) \end{bmatrix}}{s^2 + s \cdot \frac{r_E + r_c + F_m U_E + \frac{1}{LC}}{L}} + \begin{bmatrix} F_m q_i I_o & 0 \\ 0 & 0 \end{bmatrix} \quad (10)$$

$$\begin{bmatrix} G_{ci} \\ G_{co} \end{bmatrix} = \frac{\begin{bmatrix} F_m U_E (D - F_m I_o)s \\ F_m U_E (1 + sr_c C) \end{bmatrix}}{s^2 + s \cdot \frac{r_E + r_c + F_m U_E + \frac{1}{LC}}{L}} + \begin{bmatrix} F_m I_o \\ 0 \end{bmatrix} \quad (11)$$

$$\begin{aligned} r_E &= r_L + Dr_{ds} + D'r_d \\ U_E &= U_{in} + U_D + I_o(r_d - r_{ds}) \end{aligned} \quad (12)$$

The open-loop output impedance resulting from the application of the unity-feedforward scheme can be computed from (7) letting $H_i(s)=1$, and replacing the corresponding transfer functions with those specified in (10) and (11). The resulting output impedance becomes as shown in

$$Z_{o-o-ocf} = \frac{(r_E + (1 - \frac{R_{s2}}{R_{s1}})F_m U_E + sL)(1 + sr_c C)}{LC} = \frac{1}{s^2 + s \cdot \frac{r_E + r_c + F_m U_E + \frac{1}{LC}}{L}} \quad (13)$$

According to (13), we can make the following conclusions.

If, $R_{s2} = R_{s1}$ then the unity-feedforward output impedance would resemble the output impedance of a VMC buck converter without resonant behavior, which is known to be small except at the vicinity of the resonant frequency.

If, $R_{s2} \neq R_{s1}$, then the magnitude of the output impedance would approach the magnitude of the PCMC buck converter along the increase in the match error.

If, then the phase of the output impedance would start at 180° at low frequencies, when $r_L + Dr_{ds} + D'r_d + (1 - (R_{s2}/R_{s1}))F_m(U_{in} + U_D + I_o(r_d - r_{ds})) < 0$ as explained also in. It may be obvious that the minimum low-frequency output impedance would take place, when $r_L + Dr_{ds} + D'r_d + (1 - (R_{s2}/R_{s1}))F_m(U_{in} + U_D + I_o(r_d - r_{ds})) = 0$.

If $R_{s2} < R_{s1}$, then the phase behavior of the output impedance is similar to the open-loop output impedance of the PCMC buck converter.

If the input-to-output transfer function $[G_{i0-o}, (10)]$ is small as with the optimal compensation stated above, then the source interactions would be minimal. If the compensation deviates from the optimal value (i.e., overcompensation), then the load interactions may be reflected into the input side according to (3) and (5). The key factor in this sense would be the output-to-input transfer function ($T_{oi-o-ocf}$), which may be given as (14). The overcompensation means that the duty-ratio gain (F_m) decreases compared to the optimal compensation, and as a consequence, the poles and zeros of (14) would approach each other. This means that the magnitude of $T_{oi-o-ocf}$ approaches unity also at low frequencies boosting the load reflections into the input side $[(4.3), Y_{in-o} + (G_{i0-o} T_{oi-o}) / (Z_L + Z_{o-o})]$. In a PCMC buck converter, the magnitude of would decrease along the decrease in F_m as may be concluded according to

(15), and therefore, the load reflections would be reduced

$$T_{oi-o-ocf} = \frac{(D-F_m I_o)(1+s(r_c + \frac{R_{s1} R_{s2} F_m U_E}{L}))}{s^2 + s \frac{r_E + r_c + F_m U_E}{L} + \frac{1}{LC}} + \frac{R_{s2} F_m I_o}{R_{s1}} \quad (14)$$

$$T_{oi-o} = \frac{(D-F_m I_o)(1+s r_c)}{s^2 + s \frac{r_E + r_c + F_m U_E}{L} + \frac{1}{LC}} \quad (15)$$

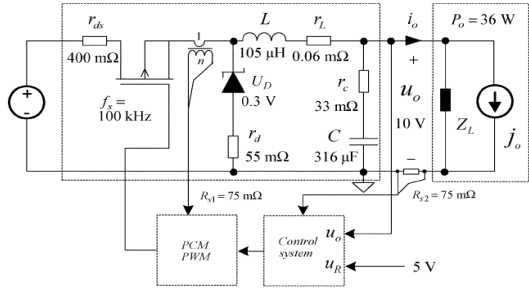


Fig. 4. Buck converter.

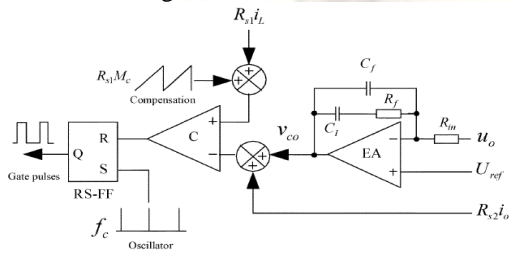


Fig 5 Simplified block diagram illustrating the implementation of the overall control system.

The authentic unity-feed forward PWM modulator and control system corresponding to Fig.4 are shown in Fig.5. The control-block diagram in Fig.5 clarifies the overall control system implementation, where the error-amp (EA) feedback elements. A constant-current source is used to create a linear compensation ramp [i.e., $R_{s1} M_c$, Fig.5].

V. Simulation Measurements

The VMC, PCMC, and PCMC-OCF buck converters used for the Simulation frequency and time-domain measurements are built by using the same power stage shown in Fig.6, Fig.7, and Fig.8. The control system is changed accordingly to the type of converter.

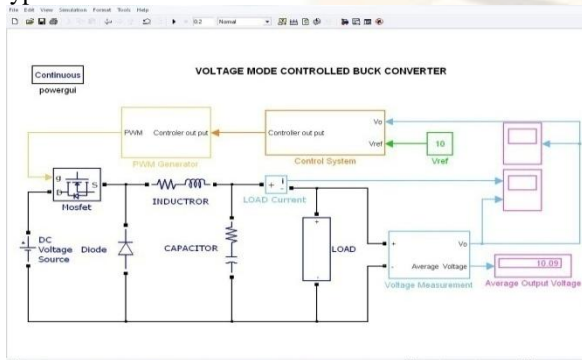


Fig.6 Simulation Circuit of VMC buck Converter

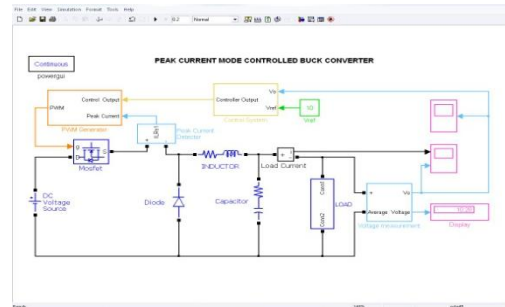


Fig.7 Simulation Circuit of PCMC buck Converter

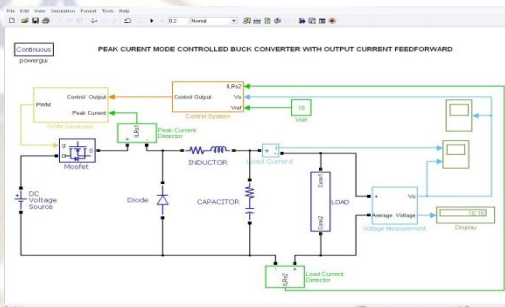


Fig.8 Simulation Circuit of PCMC-OCF buck Converter

i) Internal Nominal Dynamics

The voltage-loop gains of the converters are shown in Fig.9 for VMC and Fig.10 for PCMC and PCMC-OCF. Fig.9 and Fig.10 shows clearly that the load-current feed forward does not change the nominal loop gain as predicted in (7).

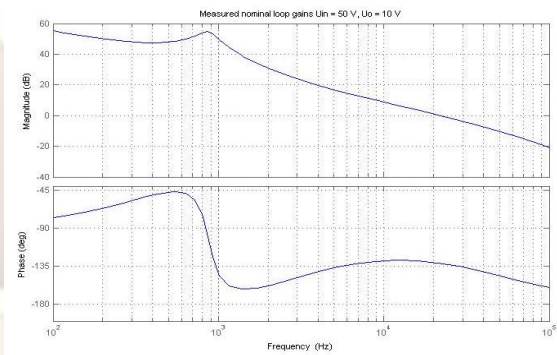


Fig.9 Voltage-loop gain of VMC buck Converter

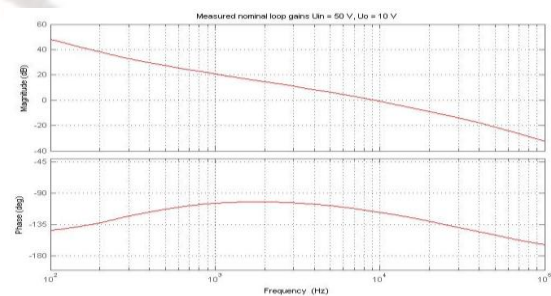


Fig.10 Voltage-loop gain of PCMC and PCMC-OCF buck Converter

The measured nominal open-loop output impedances are shown in Fig. 11, Fig. 12 and Fig. 13 of VMC, PCMC, PCMC-OCF respectively. The effect of the load-current feedforward is obvious.

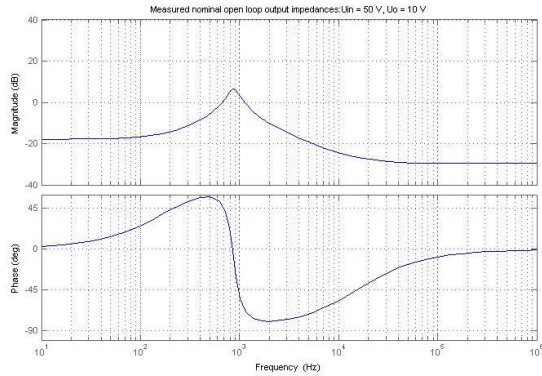


Fig 11 Open loop output impedance of VMC buck Converter

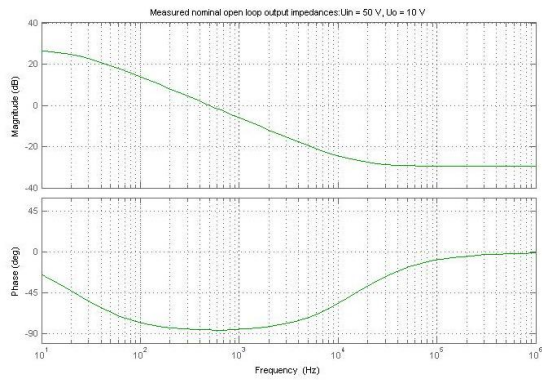


Fig 12 Open loop output impedance of PCMC buck Converter

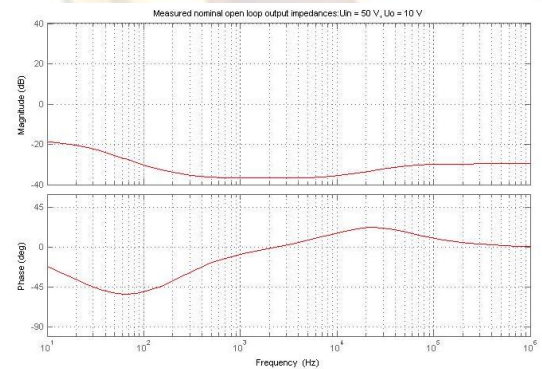


Fig 13 Open loop output impedance of PCMC-OCF buck Converter

All the converters were subjected to a constant-current-type load change from 0.5 to 2.75. Even if the loop-gain-related dynamical parameters are virtually identical, the output-voltage responses are quite different as shown in Fig. 14, Fig. 15 and Fig. 16 for VMC, PCMC, PCMC-OCF respectively.

The differences can be explained by means of the differences in the open-loop output impedances.

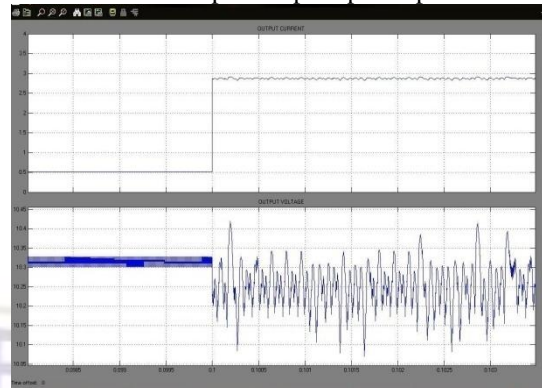


Fig. 14 Output-voltage responses to a load change from 0.5 to 2.75 A of VMC buck converter

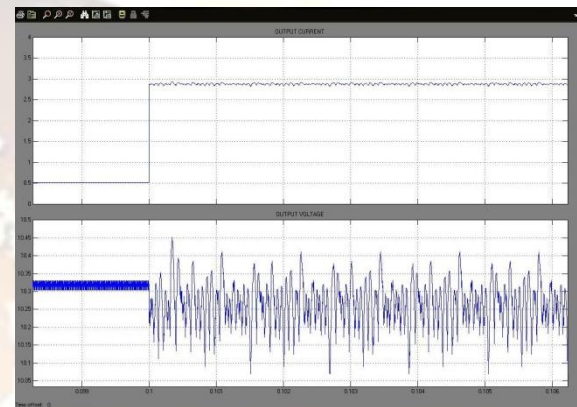


Fig. 15 Output-voltage responses to a load change from 0.5 to 2.75 A of PCMC buck converter

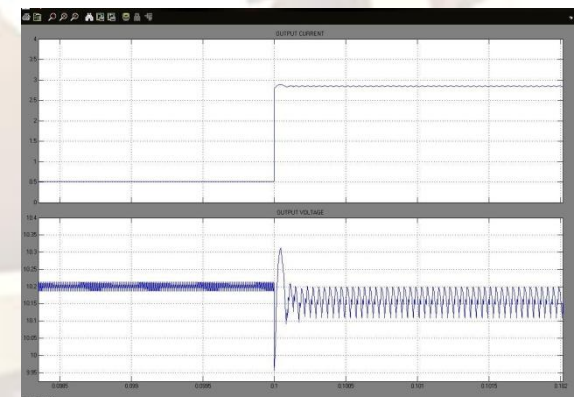


Fig. 16 Output-voltage responses to a load change from 0.5 to 2.75 A of PCMC-OCF buck converter

ii) Effect of Mismatch in Sensing Resistors

The current-sensing-resistor ratio R_{s2}/R_{s1} (Fig 18) was varied and the open-loop output impedance of the PCMC-OCF converter was measured. The behavior of the internal open-loop output impedance follows the rules implied in (Fig 18).

The PCMC-OCF converter was subjected to the same constant-current-type load change as in Fig. 14, Fig. 15 and Fig. 16 for VMC, PCMC, PCMC-

OCF respectively. when the resistor ratio is 1.1 or 10%. The corresponding output-voltage response is shown in Fig. 17(bottom subplot) compared to the response at the ideal resistor ratio (upper subplot). The phase behavior of the open-loop output impedance (i.e., low-frequency phase close to 180) results in a slight overshoot in the response.

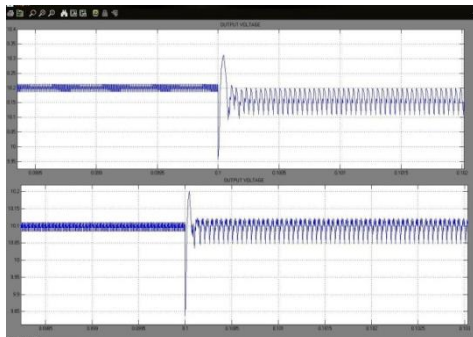


Fig 18 Output-voltage response of PCMC-OCF converter to a constant-current type load change from 0.5 to 2.75 A at the input voltage of 50 V, when $R_{s2}/R_{s1}=1$ (upper subplot) and $R_{s2}/R_{s1}=1.1$ (bottom subplot).

5.2.3 Load Sensitivity

It was shown in Section II that the direct load interactions would be reflected into the converter dynamics via the open loop output impedance as depicted in (1). It is known that the impedance ratio Z_{o-c}/Z_L would predict the load-imposed instability of the converter, where Z_{o-c} is the closed-loop output impedance of the converter. As a consequence, the instability boundary in respect to the load impedance can be defined explicitly as $Z_L = -Z_{o-c}$, which means that $|Z_L| = |Z_{o-c}|$, and $\angle Z_L = \angle Z_{o-c} - 180^\circ$

$$L^1(s) = \frac{L(s)}{1 + \frac{Z_{o-c}}{Z_L}} \quad (5.1)$$

The measured closed-loop output impedances of the VMC, PCMC and PCMC-OCF converters are shown in Fig.5.14, Fig.5.15 and Fig.5.16 when $R_{s2} \approx R_{s1}$ (Fig. 5.16: 1), and $R_{s2} > R_{s1}$ (Fig. 5.16: 2). If the phase of the output impedance is 90° or higher then the converter tends to be sensitive to the capacitive or resonant-type load. If the phase is less than 90° , then the sensitivity may be addressed to the switched-mode converters with EMI filter as a load. According to Fig.20 and Fig.21, both of the converters are sensitive to converter loads at high frequencies. The match error in the sensing resistors would clearly increase the capacitive-load sensitivity of the PCMC-OCF converter and extend it up to rather high frequencies, which is more severe effect than the slight overshoot observed in the time domain transient behavior in Fig.22

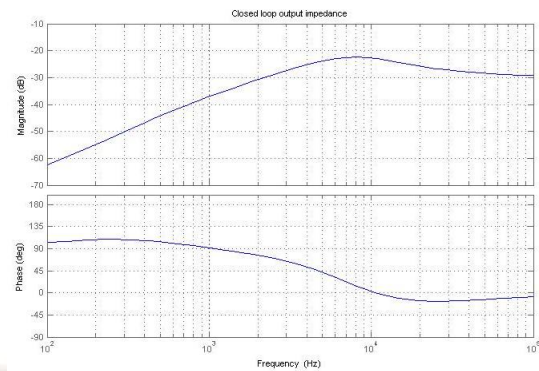


Fig 19. Closed-loop output impedances of VMC buck converters

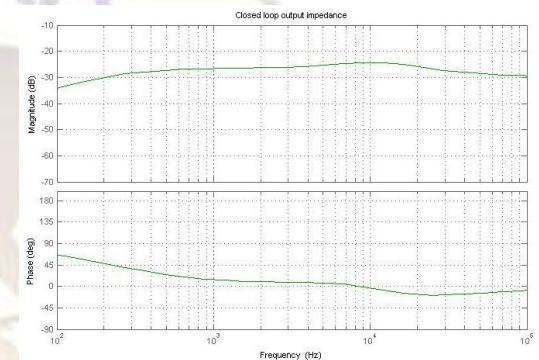


Fig 20. Closed-loop output impedances of PCMC buck converters

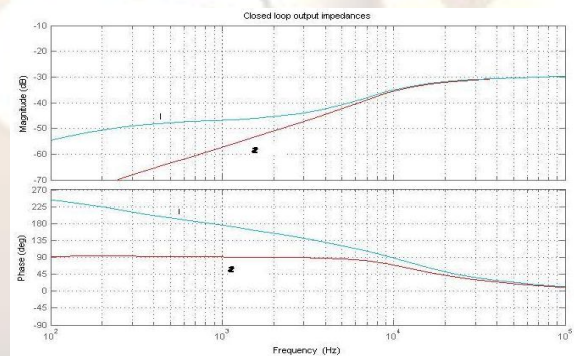


Fig 21. Closed-loop output impedances of PCMC-OCF buck converters

It was stated earlier that the difference in the output-current susceptibility (T_{oi-o}) between PCMC-OCF (4.14) and PCMC (4.15) converter would make the PCMC-OCF converter more susceptible to the load interaction reflected back due to changes in the open-loop input admittance. The measured output-current susceptibilities are shown in Fig. 21, Fig. 22 and Fig. 23 for VMC, PCMC, PCMC-OCF respectively. When the input-to-output transfer function (G_{10-o}) is same for both of the converters, it may be obvious that the reflected load sensitivity would be much higher in the PCMC-OCF converter than in the PCMC converter at high frequencies as discussed earlier in Section III.

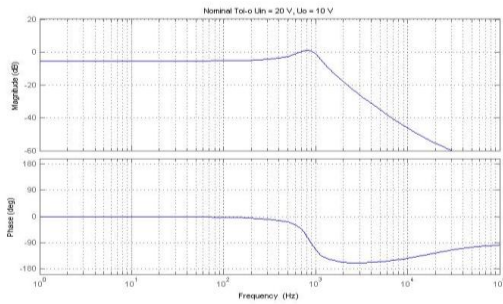


Fig 22 Open-loop output-current susceptibilities (T_{oi-o}) of VMC buck converter.

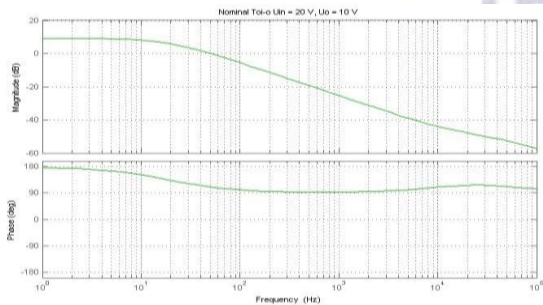


Fig 23 Open-loop output-current susceptibilities (T_{oi-o}) of PCMC buck converter.

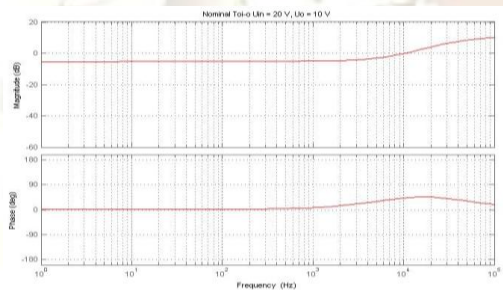


Fig 24 Open-loop output-current susceptibilities (T_{oi-o}) of PCMC-OCF buck converter.

VI. CONCLUSION

The dynamical effect of unity-load-current feed forward in a PCMC buck converter was investigated. A sound theoretical formulation was defined and applied to obtain an analytical description of the internal dynamics of such a converter. The dynamical characterization proved the previous findings but introduced also new earlier unobserved features. It was stated that a PCMC-OCF buck converter may possess both high invariance to supply and load side interactions, if an optimal slope compensation and a match in the inductor- and load-current sensing resistors exist. The match error in the sensing resistors would increase the open-loop output impedance and make the converter more sensitive to load interactions. It may be possible to maintain the match error sufficiently small, and therefore, the unity output-current-feed forward would provide a method to significantly reduce the load and supply side interactions.

REFERENCE

- [1]. B.Choi, B.H.Cho, and S.-S. Hong, "Dynamics and control of DC-to-DC converters driving other converters downstream," *IEEE Trans. Circuits Syst. I*, vol. 46, no. 10, pp. 1240–1248, Oct. 1999.
- [2]. B. Choi, B. J. Kim, B. H. Cho, and C. M.Wildrick, "Designing control loop for DC-to-DC converters loaded with unknown AC dynamics," *IEEE Trans. Ind. Electron.*, vol. 49, no. 4, pp. 925–932, Aug. 2002.
- [3]. N. Mohan, T. M. Undeland, and W. P. Robbins, *Power Electronics: Converters, Applications, and Design*. New York: Wiley, 1995.
- [4]. Matti Karppanen, Teuvo Suntio, Member, IEEE, and Mika Sippola "Dynamical Characterization of Input-Voltage Feedforward-Controlled Buck Converter" *IEEE TRANSACTIONS ON INDUSTRIAL ELECTRONICS*, VOL. 54, NO. 2, APRIL 2007
- [5]. R. Redl and N. O. Sokal, "Near-optimum dynamic regulation of DC-DC converters using feed-forward of output current and input voltage with current-mode control," *IEEE Trans. Power Electron.*, vol. PE-1, no. 3, pp. 181–191, Jul. 1986.
- [6]. G. K. Schoneman and D. M. Mitchell, "Output impedance considerations for switching regulators with current-injected control," *IEEE Trans. Power Electron.*, vol. PE-4, no. 1, pp. 25–35, Jan. 1989.
- [7]. P. Li and B. Lehman, "Performance prediction of DC-DC converters with impedances as loads," *IEEE Trans. Power Electron.*, vol. 19, no. 1, pp. 201–209, Jan. 2004.
- [8]. Timothy.l.skvarenina, *The power electronics hand book industrial electronics series*.CRC press.
- [9]. M.H. Rashid, *Power electronics: Circuits devices and applications*, prentice hall of India, 2nd edition, 1998.
- [10]. M.H. Rashid, *Power electronics hand book*, academic press.



Completed B.Tech. Electrical & Electronics Engineering in 2007 and worked as Asst. Prof in SANA Engineering college and Kodad institute of technology and science for women, kodad presently he is M.Tech Schlor at Aurora engineering college Bhonagiri, Andhrapradesh. His area of interests are DC-DC converters and Multilevel inverters